Modelization of cracks with hydro-mechanical coupling in Summarized saturated porous environment

:

One proposes a new element of joint allowing to model in 2D discontinuities with coupling-hydromechanics. This element is used to net a crack or a way of crack in a mesh of voluminal elements THM classics in the case of a saturated porous material. It makes it possible to model the behavior of a water seal or a crack under fluid pressure.

One presents here the constitutive equations of the mechanics and the hydraulics in crack as well as the corresponding constitutive laws. One also details the adopted discretization and the vector internal force and the tangent operator introduced into operator `STAT_NON_LINE`.

Contents

Contents

1 Introduction

One presents here a model of discontinuity in porous environment saturated with hydro-mechanical coupling which gives an account of the following coupled phenomena:

- the preferential flow of the fluid intersticiel in the joint, which depends on the opening of crack,
- the exchanges of fluid between the joint and the porous environment,
- the strain of the solid mass and the crack opening under the action of the crack pressure,
- propagation of crack.

According to the constitutive law chosen, this model makes it possible to model the propagation of crack or simply the behavior of a water seal already completely open. This element of joint rests on the formulation of the elements of joints already present in *Code_Aster* in classical mechanics [dj]. Hydraulic degrees of freedom are added in order to and the take into account flow in crack exchanges of fluid with the porous solid mass.
The propagation is represented by a model of cohesive zone and one uses the regularized cohesive models of the mechanical elements of joints. In order to model the behavior of the water seals completion opened, one introduces the constitutive law of Bandis.
The crack way is discretized by these elements of joint while the rest of structure is with a grid by voluminal elements THM already existing in *Code_Aster* [dthm].

One describes here the conservation equations hydraulic and mechanical along discontinuity, the corresponding constitutive laws, as well as the numerical integration of these equations.

This work fits in the frame of the GNR MoMas (program TB5, Excavation Ramming Zones).

2 Presentation of the problem

2.1 Assumptions

One considers a porous environment, noted Ω at the current time and whose border is noted $\partial\Omega$. This volume is separate in two parts Ω^+ and Ω^- by an interface Γ . All quantities in Ω^+ (resp. Ω^-) of one + (reps are subscripted. of one -).

One under investigation limits porous environment saturated with two dimensions.

2.2 Notations

2.2.1 Mechanical magnitudes

the field of displacement in the solid mass and the discontinuity of displacement through crack are noted respectively $\boldsymbol{u}=\begin{pmatrix} u_x \\ u_y \end{pmatrix}$ and $[\![\boldsymbol{u}]\!]=\begin{pmatrix} [\![u_x]\!] \\ [\![u_y]\!] \end{pmatrix}$.
The total stress and the effective stress are noted respectively $\boldsymbol{\sigma}$ and $\boldsymbol{\sigma}'$ in the solid mass and $\boldsymbol{\tau}$ $\boldsymbol{\tau}'$ on the interface.

2.2.2 Hydraulic quantities

the pressure of pore of the fluid intersticiel is noted p^+ and p^- in the solid masses surrounding crack. The fluid pressure in crack is noted p . The gradient of pressure in the solid masses is noted ∇p^+ or ∇p^- . The longitudinal gradient of the pressure of the crack is noted $\nabla_l p$ and defined by

$$\nabla_l p = \nabla p - \frac{\partial p}{\partial n}\boldsymbol{n} \quad (2.2.1)$$

where $\boldsymbol{n}$ is the norm with the interface.

The mass fluid contributions are noted m in the solid mass (unit: $M.L^{-3}$). In crack, they are noted w (unit: $M.L^{-2}$) and are integrated on the thickness ε of crack:

The mass hydraulic flux in the solid mass is noted $\boldsymbol{M}$ (unit: $M.T^{-1}.L^{-2}$). In crack, the mass hydraulic flow is noted W (unit: $M.T^{-1}.L^{-1}$).

ε is the opening of crack and is thus connected to the jump of normal displacement by

$$\varepsilon = \varepsilon_0 + [\![\boldsymbol{u}]\!].n \quad (2.2.2)$$

Where ε_0 is the initial thickness.

3 Continuous equations

3.1 Mechanics

3.1.1 Constitutive equations

the formulation of the models to cohesive zone and their numerical integration are presented in documentation of reference [R7.02.11]. One makes a very short recall here of it.

One seeks the field of displacement $\boldsymbol{u}$ to the equilibrium by minimization of the energy

$$E(\boldsymbol{u}) = \int_{\Omega/\Gamma} \phi(\boldsymbol{\varepsilon}(\boldsymbol{u}))\, d\,\Omega - W^{\text{ext}}(\boldsymbol{u}) + \int_{\Gamma} \Psi([\![\boldsymbol{u}]\!])\, d\,\Gamma \quad (3.1.1)$$

where ϕ is the density of mechanical energy voluminal, W^{ext} is the work of the forces outsides and Ψ is the density of energy of surface.

The data of Ψ characterizes the structural mechanics behavior of the interface. It is expressed by a cohesive model which connects the force of cohesion $\boldsymbol{\tau}$ which is exerted on the lips of crack to the jump of displacement by:

$$\boldsymbol{\tau} = \frac{\partial \Psi}{\partial [\![\boldsymbol{u}]\!]} \quad (3.1.2)$$

In addition, the assumption of the effective stresses is made. In the solid mass, the tensor forced total is broken up into:

$$\boldsymbol{\sigma} = \boldsymbol{\sigma}' + \sigma_p \boldsymbol{I} \quad (3.1.3)$$

where $\boldsymbol{\sigma}'$ indicates the effective stress and σ_p the hydraulic stress.

On discontinuity, the vector forced total is broken up into:

$$\boldsymbol{\tau}=\boldsymbol{\tau}'+\tau_p \boldsymbol{n} \quad (3.1.4)$$

where $\boldsymbol{\tau}'$ the effective stress indicates.

3.1.2 Constitutive laws

3.1.2.1 Effective stresses

In the solid mass, one makes the assumption of the effective stresses of Biot for the saturated mediums, by introducing the hydraulic stress σ_p function of the pressure p (in fact p^+ or p^- in the solid mass) such as:

$$\sigma_p=-b\,p \quad (3.1.5)$$

where b is the coefficient of Biot of the material.

On discontinuity, in the frame of a model of cohesive zone, one distinguishes three zones:

- an open zone where the total stress on the lips is equal to $p\,\boldsymbol{n}$;
- a zone of transition enters the open medium and the healthy medium. In this zone, one observes the appearance of microfissuring and plasticity. One thus makes the plastic assumption of incompressibility of the matrix and it is the effective stress of Terzaghi which controls the opening of the zone. The total stress is then written

$$\boldsymbol{\tau}=\boldsymbol{\tau}'-p\,\boldsymbol{n} \quad (3.1.6)$$

- a healthy zone where there are dependancy and not interpenetration of the lips. As long as the value of the stress remains lower than the critical stress, the opening remains null.

One thus makes the assumption, in coherence with the behavior of these three zones, that

$$\tau_p=-p \quad (3.1.7)$$

3.1.2.2 cohesive Models

The model presented here is compatible with the cohesive models whose energy is regularized into zero:

- CZM_LIN_REG,
- CZM_EXP_REG.

These models make it possible to take into account:

- Noninterpenetration of the crack lips by penalization;
- Crack propagation by a lenitive model;
- The irreversibility of cracking.

The material parameters of the interface are the critical stress with the fracture σ_c and the energy of fracture G_c . The numerical parameters are the parameter of regularization of energy PENA_ADHERENCE and the parameter of penalization of interpenetration PENA_CONTACT.

3.1.2.3 Model of Bandis

In this case, the model of joint does not take into account the crack propagation. The joint separates two solid masses while being open all length and is simply equipped with a model which connects the opening to the effective stress.

In the case of the empirical model of Bandis[bandis], the relation between the normal effective stress τ'_n and the normal crack closing $U=U_{\max}-\varepsilon$ (where U indicates $[\![\boldsymbol{u}]\!].\boldsymbol{n}$) is given by

$$d\tau'_n=-K_{\mathrm{ni}}\frac{dU}{\left(1-\frac{U}{U_{max}}\right)^{\gamma}} \qquad (3.1.8)$$

where U_{max} is the asymptotic closing of crack, K_{ni} the normal initial stiffness of discontinuity and γ an empirical coefficient which varies between 2 and 6 and which depends on the surface roughness of the joint. The constitutive law (3.1.8) is represented in figure 3.1.1.

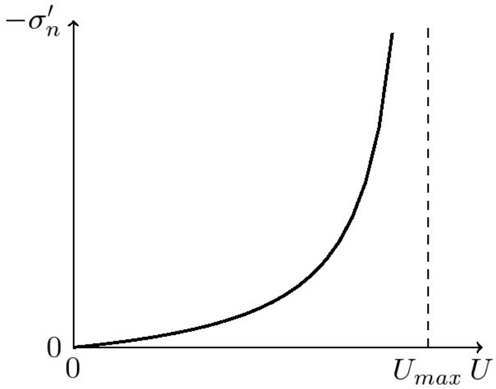

Illustration 3.1.1: Model of Goodman: curve force-closing

In the tangential direction, the behavior is supposed to be elastic.

$$\tau'_t=\tau_t=K_t[\![u_t]\!] \qquad (3.1.9)$$

the key word of *Code_Aster* corresponding to this model is `JOINT_BANDIS`. This key word is with being informed in `DEFI_MATERIAU` like in the behavior (in `RELATION_KIT`).

3.2 Hydraulics

3.2.1 Constitutive equations

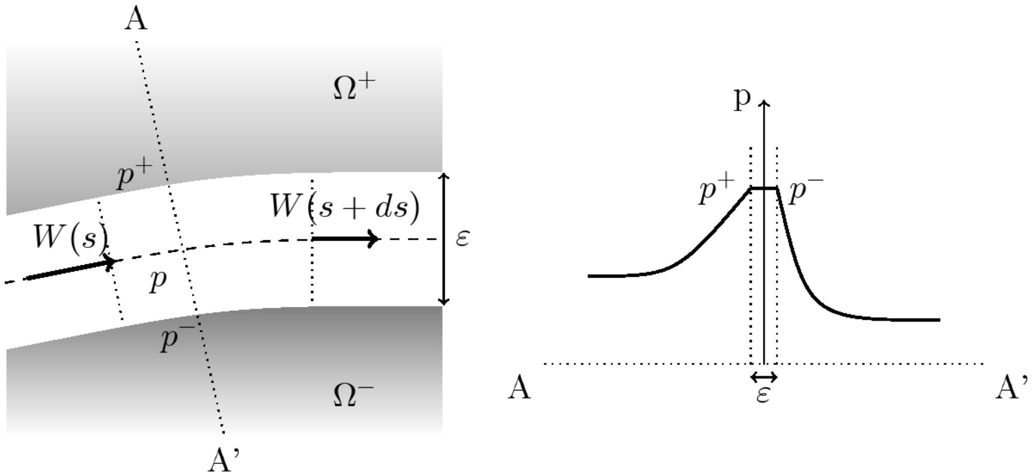

Illustration 3.2.1: conservation of the mass in crack (on the left) and typical profile of pressure through the interface (on the right)

the conservation equation of the mass in crack is written

$$\frac{\partial w}{\partial t}+\frac{\partial W}{\partial s}=0 \tag{3.2.1}$$

the thickness of crack being weak, one considers that the field of pressure is continuous through the interface. In any point of the interface, one thus has

$$p_\Gamma^+=p=p_\Gamma^- \tag{3.2.2}$$

On the other hand, flux discontinuities are authorized through the interface (see figure 3.2.1 right)

3.2.2 Constitutive laws

the mass fluid contributions in the open crack are written

$$w=\rho\,\varepsilon \tag{3.2.3}$$

Where ρ is the density of the fluid.
The evolution of the mass contributions is given by:

$$\frac{d\,w}{\rho}=\left(\frac{1}{N}+\frac{\varepsilon}{K_f}\right)d\,p+d\,\varepsilon \tag{3.2.4}$$

where K_f is the modulus of compressibility of the fluid and N the modulus of Biot of the cohesive zone.

It is considered that flow in crack is darcéen. The mass flux can thus be written

$$W=-\varepsilon\,\rho\,\lambda_H\left(\frac{\partial p}{\partial s}-\rho\,g\,\frac{\partial z}{\partial s}\right) \tag{3.2.5}$$

where λ_H is the hydraulic conductivity of crack and Z indicates the coordinate along the vertical axis. It is given by

$$\lambda_H=\frac{K(\varepsilon)}{\mu(T)} \tag{3.2.6}$$

the relation between flux and the gradient of pressure is given by the cubic model[cubiq]. The voluminal flux through crack is then written

$$\frac{W}{\rho}=-\frac{\varepsilon^3}{12\mu}\left(\frac{\partial p}{\partial s}-\rho g\frac{\partial z}{\partial s}\right) \tag{3.2.7}$$

and the intrinsic permeability K according to the opening

$$K(\varepsilon)=\frac{\varepsilon^2}{1\,2} \tag{3.2.8}$$

One notes T the transmissivity of crack, defined by

$$T=\varepsilon\lambda_H\rho=\frac{\rho\varepsilon^3}{1\,2\mu} \tag{3.2.9}$$

This model is found analytically by the model of One tenth of a poise when one studies a laminar flow between two smooth plates separated by a small ε distance in front of other dimensions. Its validity was also put in obviousness on cracks in the rocks for a broad range of parameters[cubiq].

When the crack walls are impermeable, one can of the finite elements model the solid mass with mechanical classics. In this case, the flow equation becomes singular in the part of closed and not damaged crack. One thus introduces a parameter of regularization OUV_FICT which makes it possible to have a fictitious flow in the part of closed crack. On the closed elements, one takes ε equal to OUV_FICT.

4 Mechanical variational

4.1 formulation

One notes U_{ad} all the acceptable fields of displacements, i.e. the elements of $\left(H^1(\Omega)\right)^d$ checking the boundary conditions in displacement on the part of $\partial\Omega$ supporting of such conditions.

The conditions of optimality for energy (3.1.1) give the following variational formulation:

$$\begin{cases}\boldsymbol{\sigma}=\boldsymbol{\sigma}'+\sigma_p\boldsymbol{I}\\ \boldsymbol{\tau}=\boldsymbol{\tau}'-p\,\boldsymbol{n}\\ \int_{\Omega\backslash\Gamma}\boldsymbol{\sigma}:\boldsymbol{\epsilon}(\hat{\boldsymbol{u}})\,d\Omega+\int_\Gamma\boldsymbol{\tau}.[\![\hat{\boldsymbol{u}}]\!]\,d\Gamma=W_{ext}(\hat{\boldsymbol{u}}) \qquad \forall\hat{\boldsymbol{u}}\in U_{ad}\end{cases} \tag{4.1.1}$$

4.2 Hydraulic

One notes P^{+}_{ad} (resp. P^{-}_{ad}) all the acceptable fields of pressure on Ω^{+} (resp. Ω^{-}), i.e. elements of $H^{1}(\Omega^{+})$ (resp. $H^{1}(\Omega^{-})$) checking the boundary conditions in pressure on $\partial\Omega^{+}_{P}$, the part of $\partial\Omega^{+}$ supporting boundary conditions in pressure, (resp. $\partial\Omega^{-}_{P}$). And one notes P_{ad} all the acceptable fields of pressure on Γ, i.e. the elements of $H^{1}(\Gamma)$ checking the boundary conditions in pressure on $\partial\Gamma_{P}$.

$$-\int_{\Omega^{+}}\frac{\partial m}{\partial t}\hat{p}^{+}\,d\Omega+\int_{\Omega^{+}}\boldsymbol{M}.\nabla\hat{p}^{+}\,d\Omega=\int_{\partial\Omega^{+}_{F}}\boldsymbol{F}.\boldsymbol{n}\,\hat{p}^{+}\,d\Gamma+\int_{\Gamma}q^{+}\hat{p}^{+}\,d\Gamma\quad\forall\hat{p}^{+}\in P^{+}_{ad}\tag{4.2.1}$$

$$-\int_{\Omega^{-}}\frac{\partial m}{\partial t}\hat{p}^{-}\,d\Omega+\int_{\Omega^{-}}\boldsymbol{M}.\nabla\hat{p}^{-}\,d\Omega=\int_{\partial\Omega^{-}_{F}}\boldsymbol{F}.\boldsymbol{n}\,\hat{p}^{-}\,d\Gamma+\int_{\Gamma}q^{-}\hat{p}^{-}\,d\Gamma\quad\forall\hat{p}^{-}\in P^{-}_{ad}\tag{4.2.2}$$

$$-\int_{\Gamma}\frac{\partial w}{\partial t}\hat{p}\,d\Gamma+\int_{\Gamma}W\,\nabla_{l}\hat{p}\,d\Gamma+\int_{\Gamma}\left(q^{+}+q^{-}\right)\hat{p}\,d\Gamma=\int_{\partial\Gamma_{F}}\boldsymbol{F}.\boldsymbol{n}\,\hat{p}\,ds\quad\forall\hat{p}\in P_{ad}\tag{4.2.3}$$

$$\int_{\Gamma}\left(p^{+}-p\right)\hat{q}^{+}\,d\Gamma=0\qquad\forall\hat{q}^{+}\in H^{-1}(\Gamma)\tag{4.2.4}$$

$$\int_{\Gamma}\left(p^{-}-p\right)\hat{q}^{-}\,d\Gamma=0\qquad\forall\hat{q}^{-}\in H^{-1}(\Gamma)\tag{4.2.5}$$

4.3 temporal Discretization

One adopts a discretization in implicit time. The subscripted notations by n are the quantities at the beginning of time step and those subscripted by $n+1$ are the quantities at the end of time step.

Time step is noted $\Delta t=t_{n+1}-t_{n}$.

Thereafter, in the absence of accuracy, the nonsubscripted notations will indicate the quantities at the end of time step.

5 Construction of an element of joint

the trajectory of crack Γ is a priori defined, one can thus discretize it by elements of joint. The subdomains Ω^{+} and Ω^{-}, located on both sides of Γ, are discretized by voluminal elements THM classics[dthm] so that their nodes with the interface coincide.

5.1 Degrees of interpolation of the degrees of freedom

the element of joint with hydro-mechanical coupling takes again the mechanical formulation of the classical elements of joint (but while passing from a linear element to a quadratic element) and interacts with elements THM neighbors. The degrees of interpolation of degrees of freedom is thus chooses in coherence with these close elements.

In order to be compatible with elements THM of the solid mass:

- displacements are interpolated quadratically ($P2$ - continuous)

- the pressures are interpolated linearly ($P1$ - continuous).

A degree of freedom which does not preexist in any of the two preceding elements appears in the formulation. It is the hydraulic multiplier of Lagrange (variables q^+ and q^- in the variational equations 4.2.1 to 4.2.5). The degree of interpolation of these hydraulic Lagrange multipliers must be chooses so as to observe a discrete condition LBB. They are thus taken constant by element.

5.2 Description of the element

the built element is of thickness null and one nets the group of the crack way with this element. The lower and higher edges are connected to the rest of structure. The flow of the fluid along crack is written along medium plane element (in gray on figure 5.2.1).

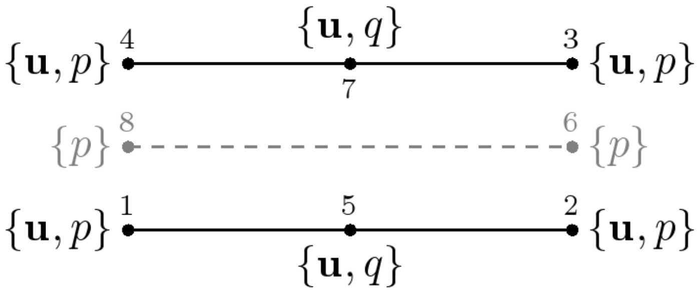

Illustration 5.2.1: "Burst" sight of the element of joint with hydro-mechanical coupling and without propagation

6 Algorithm of resolution

the variational problem (4.1.14.2.5) can be written in the form:

$$\boldsymbol{F}(\boldsymbol{U})=\boldsymbol{L}^{int}(\boldsymbol{U})-\boldsymbol{L}^{meca}=0 \tag{6.1}$$

where $\boldsymbol{U}$ indicates generalized displacements.

The associated tangent operator is noted $D\boldsymbol{F}=\frac{\partial \boldsymbol{F}}{\partial \boldsymbol{U}}$.

6.1 Generalized stresses and strains

One notes $\boldsymbol{U}^{el}$ the vector of the nodal unknowns on the element el, $\boldsymbol{E}_{pi}^{el}$ the vector of the strains generalized at the point of integration pi of the element el, $\boldsymbol{\Sigma}_{pi}^{el}$ the vector of the generalized stresses

$$\boldsymbol{\Sigma}_{pi}^{el}=\begin{Bmatrix} \boldsymbol{\tau}' \\ -p \\ w \\ W \\ q^{+} \\ q^{-} \\ p^{+}-p \\ p^{-}-p \end{Bmatrix}^{el} \quad (6.1.1)$$

$$\boldsymbol{E}_{pi}^{el}=\begin{Bmatrix} [\![\boldsymbol{u}]\!] \\ p \\ \nabla p \\ p^{+} \\ p^{-} \\ q^{+} \\ q^{-} \end{Bmatrix}^{el} \quad (6.1.2)$$

the generalized strains are obtained by the relation

$$\boldsymbol{E}_{pi}^{el}=\boldsymbol{Q}_{pi}^{el}.\boldsymbol{U}^{el} \quad (6.1.3)$$

where $\boldsymbol{Q}_{pi}^{el}$ is the transition matrix of the nodal degrees of freedom to the strains generalized at the point of integration pi. One calculates it starting from the shape functions and of the directional sense of the element. Indeed, mechanical displacements of each node are defined in the total reference. In order to extract from them the components norm and tangential with the element from joint, one applies a matrix of rotation $\boldsymbol{\Theta}_{pi}^{el}$ to the vectors nodal displacements.

6.2 Integration

to integrate on the element the terms of the vector, one chooses a selective integration method. This one makes it possible to avoid the numerical oscillations for the problems where the structure is subjected to a shock and where the mechanical phenomena prevail [select]. This method consists in integrating into the tops of the element the terms utilizing a derivative compared to time and integrating into Gauss points the permanent terms.

The vector internal force is written

$$\boldsymbol{L}^{int}(\boldsymbol{U})=\sum_{el}\left(\sum_{g}\omega_{g}\boldsymbol{R}_{g}^{el}(\boldsymbol{U}^{el})+\sum_{s}\omega_{s}\boldsymbol{R}_{s}^{el}(\boldsymbol{U}^{el})\right) \quad (6.2.1)$$

by noting $\boldsymbol{R}_{g}^{el}$ and the $\boldsymbol{R}_{s}^{el}$ values respectively at the Gauss point g and the top s of the nodal forces and ω_g the ω_s weights of integration respectively of g and s.

The tangent operator is written

$$D\boldsymbol{F}(\boldsymbol{U})=\sum_{el}\left(\sum_g \omega_g D\boldsymbol{F}_g^{el}(\boldsymbol{U})+\sum_s \omega_s D\boldsymbol{F}_s^{el}(\boldsymbol{U})\right) \quad (6.2.2)$$

by noting $D\boldsymbol{F}_g^{el}$ and the $D\boldsymbol{F}_s^{el}$ values respectively at the Gauss point g and the top s of the tangent operator.

The tangent operator and the nodal forces are thus calculated differently with Gauss points and the tops. On the other hand, all the components of the generalized stresses and all the local variables are calculated at the same time with Gauss points and the points of integration.

6.3 Vector internal forces: options RAPH_MECA and FULL_MECA

One adopts the following decomposition

$$\hat{\boldsymbol{E}}_{pi}^{elT}.\bar{\boldsymbol{\Sigma}}_{pi}^{el}=\bar{\boldsymbol{\Sigma}}_{\boldsymbol{u}}[\![\hat{\boldsymbol{u}}_g]\!]+\bar{\Sigma}_p\hat{p}+\bar{\Sigma}_{\nabla p}\nabla\hat{p}+\bar{\Sigma}_{p^+}\hat{p}^++\bar{\Sigma}_{p^-}\hat{p}^-+\bar{\Sigma}_{q^+}\hat{q}^++\bar{\Sigma}_{q^-}\hat{q}^- \quad (6.3.1)$$

where $\hat{\boldsymbol{E}}_{pi}^{el}=\left([\![\hat{\boldsymbol{u}}_g]\!],\hat{p},\nabla\hat{p},\hat{p}^+,\hat{p}^-,\hat{q}^+,\hat{q}^-\right)$ is a virtual generalized strain calculated from a vector virtual generalized displacement.

Starting from the discrete variational formulations and by distributing the steady terms under Gauss points and the non stationary terms at the tops of the element, one obtains:

- with Gauss points

$$\begin{aligned}
\bar{\boldsymbol{\Sigma}}_{\boldsymbol{u}}^{el} &= \tau'-p_g\boldsymbol{n}\\
\bar{\Sigma}_p^{el} &= \Delta t\,(q_g^++q_g^-)\\
\bar{\Sigma}_{\nabla p}^{el} &= \Delta t\,W\\
\bar{\Sigma}_{p^+}^{el} &= -\Delta t\,q^+\\
\bar{\Sigma}_{p^-}^{el} &= -\Delta t\,q^-\\
\bar{\Sigma}_{q^+}^{el} &= p^+-p\\
\bar{\Sigma}_{q^-}^{el} &= p^--p
\end{aligned} \quad (6.3.2)$$

- at the tops

$$\begin{aligned}
\bar{\boldsymbol{\Sigma}}_{\boldsymbol{u}}^{el} &= \boldsymbol{0}\\
\bar{\Sigma}_p^{el} &= w_n-w_{n+1}\\
\bar{\Sigma}_{\nabla p}^{el} &= 0\\
\bar{\Sigma}_{p^+}^{el} &= 0\\
\bar{\Sigma}_{p^-}^{el} &= 0\\
\bar{\Sigma}_{q^+}^{el} &= 0\\
\bar{\Sigma}_{q^-}^{el} &= 0
\end{aligned} \quad (6.3.3)$$

One has in addition:

$$\hat{\boldsymbol{U}}^{elT}.\boldsymbol{R}_{pi}^{el}=\hat{\boldsymbol{E}}_{pi}^{elT}.\bar{\boldsymbol{\Sigma}}_{pi}^{el} \quad (6.3.4)$$

what gives

$$\boldsymbol{R}_{pi}^{el}=\boldsymbol{Q}_{pi}^{elT}.\bar{\boldsymbol{\Sigma}}_{pi}^{el} \quad (6.3.5)$$

6.4 tangent Operator: options FULL_MECA and RIGI_MECA_TANG

the tangent operator at the Gauss point g is given by:

$$\frac{\partial \boldsymbol{\Sigma}_g^{el}}{\partial \boldsymbol{E}_g^{el}}=\begin{bmatrix} \frac{\partial \tau_n'}{\partial [\![u_n]\!]} & \frac{\partial \tau_n'}{\partial [\![u_t]\!]} & -1 & 0 & 0 & 0 & 0 & 0 \\ \frac{\partial \tau_t}{\partial [\![u_n]\!]} & \frac{\partial \tau_t}{\partial [\![u_t]\!]} & 0 & 0 & 0 & 0 & 0 & 0 \\ 0 & 0 & 0 & 0 & 0 & 0 & \Delta t & \Delta t \\ \Delta t\,\frac{\partial W}{\partial u_n} & 0 & \Delta t\,\frac{\partial W}{\partial p} & -\Delta t\,T & 0 & 0 & 0 & 0 \\ 0 & 0 & 0 & 0 & 0 & 0 & -\Delta t & 0 \\ 0 & 0 & 0 & 0 & 0 & 0 & 0 & -\Delta t \\ 0 & 0 & -1 & 0 & 1 & 0 & 0 & 0 \\ 0 & 0 & -1 & 0 & 0 & 1 & 0 & 0 \end{bmatrix} \quad (6.4.1)$$

the tangent operator at the top s is given by:

$$\frac{\partial \boldsymbol{\Sigma}_s^{el}}{\partial \boldsymbol{E}_s^{el}}=\begin{bmatrix} 0 & 0 & 0 & 0 & 0 & 0 & 0 & 0 \\ 0 & 0 & 0 & 0 & 0 & 0 & 0 & 0 \\ -\frac{\partial w}{\partial [\![u_n]\!]} & 0 & -\frac{\partial w}{\partial p} & 0 & 0 & 0 & 0 & 0 \\ 0 & 0 & 0 & 0 & 0 & 0 & 0 & 0 \\ 0 & 0 & 0 & 0 & 0 & 0 & 0 & 0 \\ 0 & 0 & 0 & 0 & 0 & 0 & 0 & 0 \\ 0 & 0 & 0 & 0 & 0 & 0 & 0 & 0 \\ 0 & 0 & 0 & 0 & 0 & 0 & 0 & 0 \end{bmatrix} \quad (6.4.2)$$

the tangent operator at the point of integration pi is finally given by:

$$D\,\boldsymbol{F}^{el}_{pi}=\boldsymbol{Q}^{elT}_{pi}\cdot\frac{\partial\boldsymbol{\Sigma}^{el}_{pi}}{\partial\boldsymbol{E}^{el}_{pi}}\cdot\boldsymbol{Q}^{el}_{pi} \quad (6.4.3)$$

6.5 Vector nodal forces: option FORC_NODA

option FORC_NODA is used by STAT_NON_LINE at the time of the phase of prediction.

In the point of integration pi, the vector nodal forces at time $n+1$ is defined by:

$$\boldsymbol{F}^{el}_{pi,n+1}=\boldsymbol{Q}^{elT}_{pi}\cdot\bar{\boldsymbol{S}}^{el}_{pi} \quad (6.5.1)$$

where $\bar{\boldsymbol{S}}^{el}_{pi}$ is null at the tops and is given to Gauss points by:

$$\begin{aligned}
\bar{\boldsymbol{S}}^{el}_{\boldsymbol{u},n+1} &= \boldsymbol{\tau}_{g,n}-p_{g,n}\boldsymbol{n}\\
\bar{S}^{el}_{p,n+1} &= \Delta t\,(q^{+}_{g,n}+q^{-}_{g,n})\\
\bar{S}^{el}_{\nabla p,n+1} &= \Delta t\,W_{g,n}\\
\bar{S}^{el}_{p^{+},n+1} &= -\Delta t\,q^{+}_{g,n}\\
\bar{S}^{el}_{p^{-},n+1} &= -\Delta t\,q^{-}_{g,n}\\
\bar{S}^{el}_{q^{+},n+1} &= p^{+}_{g,n}-p_{g,n}\\
\bar{S}^{el}_{q^{-},n+1} &= p^{-}_{g,n}-p_{g,n}
\end{aligned} \quad (6.5.2)$$

6.6 Local variables

As for the classical models of THM, the variables of 1 with $NVIM$ ($NVIM$ depend on the mechanical constitutive law used) relate to the model of mechanics used. The following local variables are:

- V_{NVIM+1} : $\rho-\rho_0$, variation of the density
- V_{NVIM+2} : ε , opening of crack.
-

7 Validation

the following table recapitulates the cases tests of validation of the models presented in this note.

Titrate	Name of the test	Documentation	Models	axisymmetric
Model Modelization of a joint with hydraulic coupling.	wtna111	V7.33.11	AXIS_JHMS	JOINT_BANDIS
Déplétion of a tank	wtnp125	V7.32.125	PLAN_JHMS	JOINT_BANDIS
Injection of gas in a porous environment fractured	wtnp126	V7.32.126	PLAN_JHMS	JOINT_BANDIS
Tests of splitting per corner of the concrete under fluid pressure	wtnp128	V7.32.128	PLAN_JHMS	JOINT_BANDIS CZM_LIN_REG CZM_EXP_REG

8 Bibliography

[1] LAVERNE, J., “Finite elements of joint in 2D and 3D”, Handbook of reference of Code_Aster, [R3.06.09]
[2] CHAVANT C., “Modelizations THHM. General information and algorithms. ”, Handbook of reference of the Code_Aster, [R7.01.10-A]
[3] LAVERNE J., “cohesive Constitutive laws: CZM_xxx_xxx and control of the loading”, [R7.02.11]
[4] BANDIS, S., LUMSDEN, A.C, BARTON, N.: “Fundamentals of rock'n'roll joined strain”, 1983, Int. Day. Of Rock Mechanics and mining Science and Geomech. Abstr., 20(6), 249-68
[5] WHITERSPOON, P.A., WANG, J.S.Y. WIWAI, K., SCALE, J.E. : “Validity of cubic law for fluid flow in has deformable rock'n'roll fractures”, 1980 , Resour Toilets. Abstr., 16,1016 [6] FERNANDES
, R., CHAVANT, C., OF the SUAUG, G., “Definition of a modelization with selective integration for the couplings Thermo-Hydro-Mechanics”, Notes EDF R & D, [HT-66/05/012/A] Description

9 of the versions of the document Version

Aster Author	(S) or contributor (S), organization Description	of the modifications 2/10/10
02/10/10	initial	Text